

A method of core wire extraction from point cloud data of rebar

Koji Nishio	Noriyoshi Nakamura	Yuta Muraki	Ken-ichi Kobori
Osaka Institute of Technology 1-79-1, Kitayama Hirakata, Osaka JAPAN (573-0196), Koji.a.nishio@oit.ac.jp	Osaka Institute of Technology 1-79-1, Kitayama Hirakata, Osaka JAPAN (573-0196), nakamura_noriyoshi@gg l.is.oit.ac.jp	Osaka Institute of Technology 1-79-1, Kitayama Hirakata, Osaka JAPAN (573-0196), Yuta.muraki@oit.ac.jp	Osaka Institute of Technology 1-79-1, Kitayama Hirakata, Osaka JAPAN (573-0196), Kenichi.kobori@oit.ac.jp

ABSTRACT

In recent years, reinforced concrete has been widely used as a building material having high strength. However, when the arrangement of the reinforcing bars embedded in the inside are not correct, there is a problem that the strength drops greatly. Therefore, when use reinforced concrete, it is necessary to confirm whether the reinforcing bars are correctly arranged. In this paper, we propose a method of thinning of point clouds scanned by range scanner from reinforcing bars, and extracting the core wires of point clouds by introducing a concentration distribution function. This process moves points according to a gradient field of a concentration field. In addition, we conducted an experiment to confirm the effectiveness of the proposed method. As a result of the experiment, it was confirmed that the core wires can be extracted from the point clouds of the reinforcing bars.

Keywords

point cloud, thinning, core wire extraction, reinforced concrete and density distribution

1. INTRODUCTION

In recent years, reinforced concrete is widely used as a building material having high strength. However, reinforced concrete has a problem that the strength drops greatly when the number and arrangement of reinforcing bars embedded in the reinforced concrete are not correct. Therefore, in a construction using reinforced concrete, it is important to confirm whether the reinforcing bars are correctly arranged. Currently, the confirmation process is performed manually by the human eye, requiring a lot of time and possibly causing human error.

Therefore, in this paper, we propose a method to extract and reveal core wires of rebar from point cloud data scanned by a range scanner.

However, since many noise is included in the point cloud data, it is difficult to apply the previous core line extraction method. Therefore, in the proposed method, firstly, the influence of noise is reduced by thinning the point cloud data, and then the core line extraction is performed.

In the thinning process, we introduce a concentration distribution function to define a density field. This estimates the position where the core lines of the

reinforcing bars exist and converges the point cloud data there.

In the process of extracting the core line, core line candidates are generated from the density field and classified into core or non-core wires using information of point cloud data thinned.

2. Extraction of core wires from the point clouds

In recent years, researches to extract core lines (skeletons) of shapes represented by point cloud data are widely performed. In Lee's method [Lee00a], a core extraction method from unorganized point cloud data is proposed. In this method, a point cloud is thinned by a simple algorithm using a local least squares method, and the result is extracted as a core line of a point cloud. In the method of least squares, there is a problem that it is necessary to appropriately set the range to which the processing is applied. However, in this method, the problem is solved by introducing a minimum spanning tree. In addition, by applying the cylindrical shape to the least squares method with the method of Luk'acs et al. [Luk98a], it is said that a good core extraction result can be obtained for a shape like a reinforcing bar. However, this method is very weak against noise and it is

impossible to obtain good core line extraction results even with slight noise. There is also a problem that it does not correspond to a closed loop or a branched shape.

In the method of Bucksch et al. [Buc09a], the octree structure has been introduced to represent the point cloud data[Buc08a]. After that, the graph is simplified to extract the core line of the tree structure. This method is robust to noise and excellent in processing speed, however it cannot be applied to point cloud data which represents closed loop shape because it uses a tree structure.

Cao et al. [Cao10a] proposed a method to extract thin lines by shrinking the shape repeatedly using a smooth Laplacian filter. This method is applicable not only to point cloud data but also to surface data. In addition, it is possible to obtain a good extracted core line even for closed loop shape. Furthermore, it is relatively robust against noise and core line extraction is also possible from point cloud data that is partially missing if most point clouds have been acquired. However, generating the shape of the core line, it is necessary to set a plurality of weights with arbitrary values.

2.1 Problems of core wire extraction for reinforced bars

Since there are two problems in the point cloud data in this research, it is difficult to apply previous core line extraction methods for the point cloud data of reinforced bar. The first problem is that it is very noisy. The core line extraction processing in this research is targeted to point cloud data of rebar obtained by 3D scanner. However, as shown in Fig. 2.1, the point cloud data actually contains a lot of noise, and the surface of the shape cannot be acquired accurately. For this reason, the point cloud data handled in this study is different in shape from general point cloud data, and it is difficult to extract the core line by previous methods. The second problem is that the point cloud data of the rebar includes closed loop topology. In the point cloud data of reinforcing bars, as the reinforcing bars intersect each other, the point cloud data is distributed in a lattice pattern as shown in Fig. 2.2.

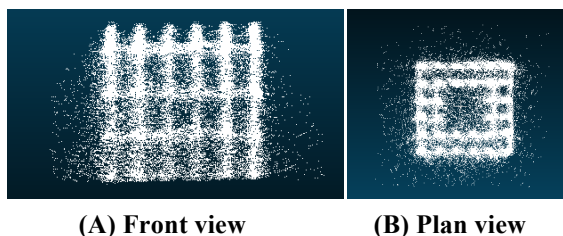


Figure 2.1 Point cloud of reinforced bars

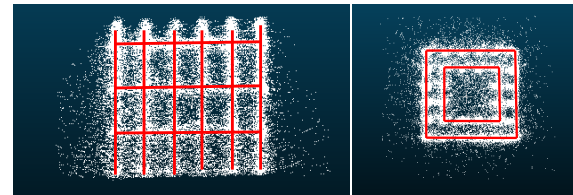


Figure 2.2 Point cloud with closed-loop distribution

3. Proposed method

In our method, a density distribution function is introduced in thinning processing to generate a density field and a vector field. Then, convergence of the point cloud according to the vector field is performed to thin the line. Thereafter, in the process of extracting the core line, intersection points of the reinforcing bars are detected from the density field and core wire candidates are generated. Then, core wires are extracted by classifying each core wire candidate into core or non-core wire from the distribution of the surrounding point cloud.

3.1 Thinning point cloud

As preprocessing for extracting the core line from the point cloud data of the reinforcing bars, thinning of the point cloud data is performed as shown in Fig.3.1.

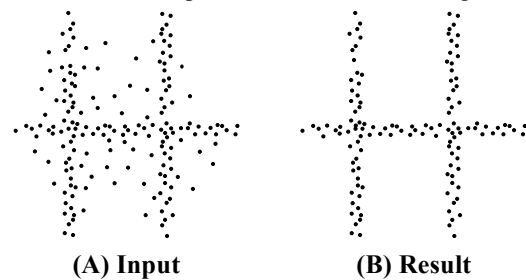
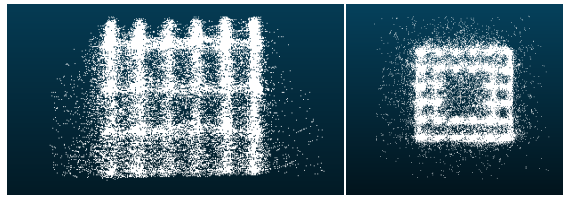


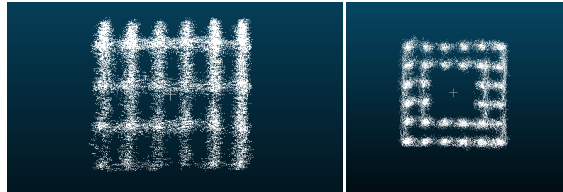
Figure 3.1 Thinning of point cloud

In this thinning process, the positions of the core lines of the reinforcing bars are estimated from the point cloud data of the reinforcing bars, and the point clouds are converged to thin lines.

In the proposed method, first, simple noise removal is performed as preprocessing. In the point cloud data scanned by the 3D scanner, points are scattered in the space, and the shape of the reinforcing bars cannot be clearly seen. However, the density of point cloud becomes high around the reinforcing bars. Therefore, it is assumed that reinforcing bars exist where the density of point clouds is relatively high, and points whose density is relatively low are removed as noise, as shown in Fig. 3.2.



(a) Before removal



(b) After removal

Figure 3.2 Noise reduction

3.1.1 Generation of density field

Because the core wire is located at the center of the reinforcing bar, in the proposed method, a concentration distribution function is introduced to estimate the position of this core line. The core lines of the reinforcing bars are near the center of the distribution of point cloud. Therefore, each point of point cloud is used as a source of the concentration distribution. The density field is generated by the density distribution function as shown in Fig. 3.3. The concentration distribution is obtained by Eq. 3.1. Where, x represents the coordinates for determining the concentration distribution value, r represents the range of the concentration distribution, and p_i represents the center coordinates of the concentration distribution, that is, the coordinates of the points of the point cloud.

$$C_m(x) = \sum_{i=1}^n \frac{(r - \|p_i - x\|)^2}{r^2} \quad (r \geq x) \quad (3.1)$$

$$C_m(x) = 0 \quad (r < x)$$

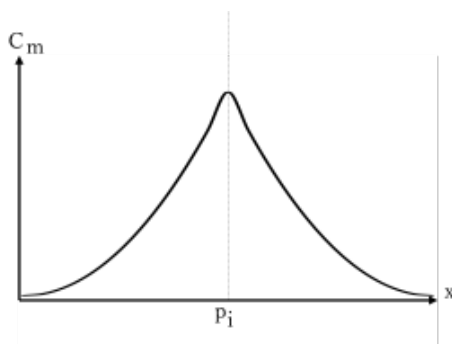
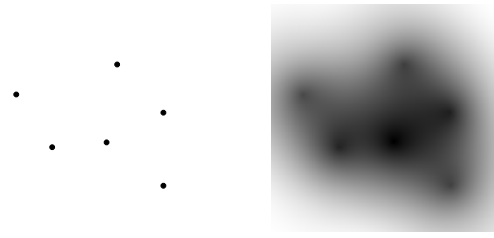


Figure 3.3 Concentration distribution function

Such concentration distribution is generated at each point of point cloud and values are added in a space where the density overlaps as shown in Fig. 3.4.



(a) Point cloud (b) Concentration field

Figure 3.4 Example of density field

3.1.2 Discretization of density field

Density field is discretized by using the voxel structure. At this time, normalization is performed so that the density value of the entire space becomes $[0, 1]$. In this paper, each voxel is referred by i, j, k sequentially allocated to the direction of each coordinate axis, and is expressed in the form of $V(i, j, k)$. It is assumed that the density value and the gradient vector is represented by $C_m(i, j, k)$ and $G(i, j, k)$ at $V(i, j, k)$ respectively.

3.1.3 Generating a vector field

Each point of the point cloud is moved according to the gradient of the density field, whereby the point cloud converges. The gradient vector $G(i, j, k)$ at $V(i, j, k)$ is obtained by the Eq. 3.2.

$$G_{(i,j,k)} = \left(\frac{\partial C_m(i,j,k)}{\partial i}, \frac{\partial C_m(i,j,k)}{\partial j}, \frac{\partial C_m(i,j,k)}{\partial k} \right) \quad (3.2)$$

3.1.4 Moving points

In this process, the movement direction and the movement distance are calculated for each voxel, and the same movement is applied to all the points in each voxel. The movement direction D and the movement distance L are obtained as follows.

First, the direction of motion is determined by Eq. 3.3. Where, T is the sum of the gradient vectors stored in each voxel in a certain range centered on the current point, and σ should be set to a value greater than 1, so as not to be affected by the fine change of the gradient vector. Thereafter, the movement direction D is determined by normalizing the magnitude of T to 1.

$$T = \sum_{l=i-\sigma}^{i+\sigma} \sum_{m=j-\sigma}^{j+\sigma} \sum_{n=k-\sigma}^{k+\sigma} G_{(l,m,n)} \quad (3.3)$$

$$D = \frac{T}{|T|}$$

Next, the movement distance L is determined by Eq. 3.4. Where, w is a width of a voxel, and p is maximum distance each point can move represented by number

of voxels. The distance of movement is proportional to the magnitude of the gradient vector. Therefore, the magnitude of the gradient vector decreases at the voxel with a high density.

$$L = w|G_{(i,j,k)}|p \quad (3.4)$$

By continuing the process described above repeatedly until the maximum movement distance of the points becomes equal to or less than the threshold value, the point cloud is thinned. However, in this state, since the concentration value becomes very high at the point where the reinforcing bars cross each other, a vector field toward the intersection of the reinforcing bars is generated. Therefore, repeating the movement of points iteratively, there is a problem as shown in Fig. 3.5. Each point of point cloud concentrates at the intersection of the reinforcing bars and the point cloud becomes discontinuous in other places.

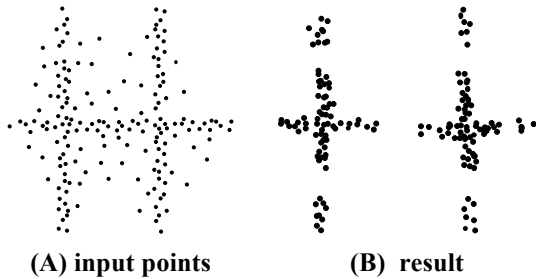


Figure 3.5 Example of the problem

As a solution to this problem, points are given spheres with radius r_s and if spheres intersect each other as shown in Fig. 3.6, a movement vector R_i which pushes back out of the radius is generated. By adding this vector to the movement process, we suppress the discontinuity of the point cloud. The vector R_i is obtained by the Eq. 3.5. Where, p is the moving point, p_i is the surrounding point, r_s is the radius of the sphere, and d is the distance between the two points.

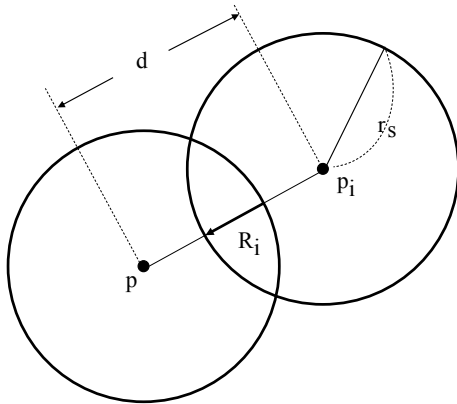


Figure 3.6 When the points are close together

$$R_i = \begin{cases} \frac{p-p_i}{|p-p_i|} (2r_s-d) & (d < 2r_s) \\ 0 & (d \geq 2r_s) \end{cases} \quad (3.5)$$

3.2 Core wire extraction

In this process, firstly, the positions of the intersection of the reinforcing bars are detected by searching for all voxels from which voxels whose density values locally have local maximum values as shown in Fig. 3.7 and extracting them as intersection points of reinforcing bars. However, as can be seen from the figure, since the density of point clouds is nonuniform, many voxels where the density value has a maximum value exist.

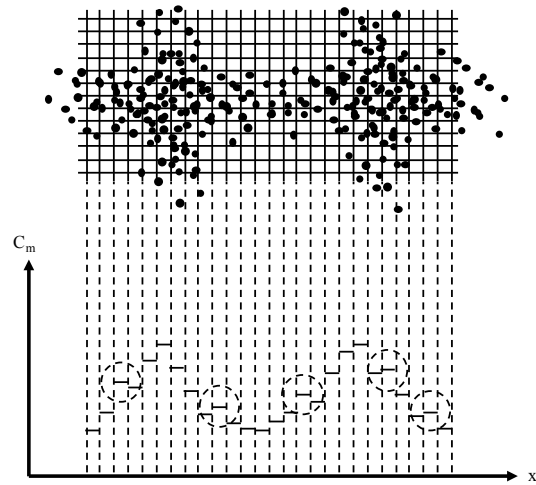


Figure 3.7 Local maximum points as an intersection points.

A voxel whose concentration value locally reaches a local maximum value is searched for and extracted as an intersection point of reinforcing bars.

Next, a core line candidate of the rebar is generated. The core line candidates are edges connecting the intersection points as shown in Fig. 3.8. However, these candidates contain **wrong things**. Therefore, it is necessary to classify these candidates into a core or non-core wire.

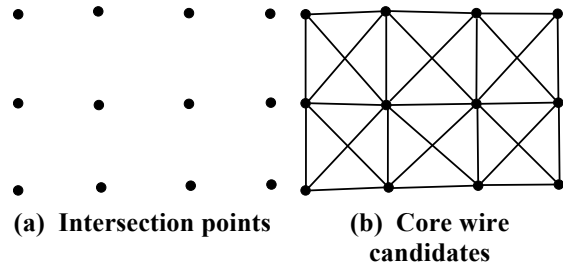


Figure 3.8 Core wire candidate

It is determined whether or not each core wire candidate is the core wire of an actual reinforcing bar by using the position information of the point cloud.

As shown in Fig. 3.9, the points are densely distributed around the core line of the reinforcing bars, and distributed sparsely in other places. Therefore, by examining the distribution of points around each core line candidate, it is considered that classification of the core or non-core wire can be performed.

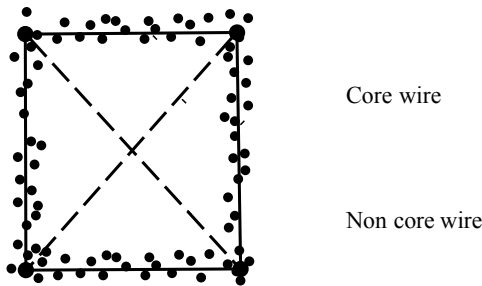


Figure 3.9 Distribution of points along the wire

First, as shown in Fig. 3.10, each point of the point cloud is projected on the line of the nearest core line candidate. Where, P_i is the point before projection, P'_i is the point after projection, P_s - P_e is a core wire candidate, n is the number of points projected on the core line candidate and pd_i is a distance between neighboring points.

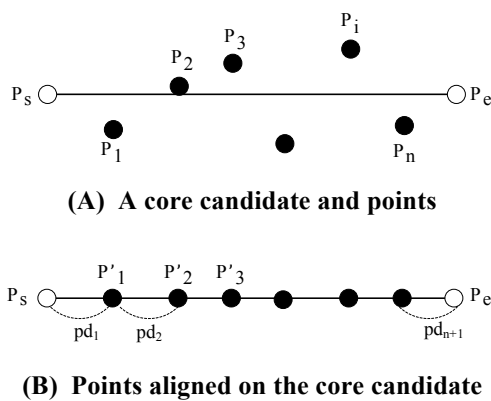


Figure 3.10 Projection of points

After that, the distance pd_{max} that is the maximum distance of pd_i s, is obtained by the Eq. 3.7.

$$pd_{max} = \max(PD) \tag{3.7}$$

$$PD = \{pd_i | i = 1, 2, \dots, n\}$$

If pd_{max} is smaller than th denoted by Eq. 3.8, the core line candidate is determined as a core line, and else it is determined as a non-core line. Where, E in the

equation is the length of the core line candidate, and ρ is a parameter of $[0, 1]$.

$$th = E \times \rho \tag{3.8}$$

$$E = |P_e - P_s|$$

The core line candidates classified by the above processing are shown in Fig. 3.11. In this figure, the core wire is indicated by a solid line, and the non-core wire is indicated by a broken line.

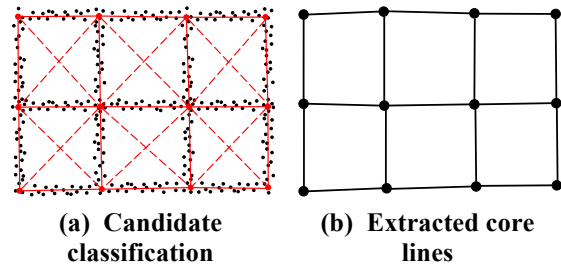


Figure 3.11 Classification and extraction result

4. Results

The point cloud captured by a 3D scanner from the reinforced bars is shown in fig. 4.1 and the final thinning result generated by our method is shown in Fig. 4.2. In this experiment, we used $128 \times 128 \times 128$ voxels, set r to 10 times the voxel width, σ to 13, p to 2.0, and r_s to 0.1.

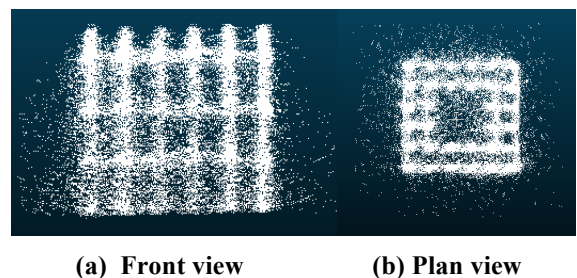


Figure 4.1 Point cloud of reinforced bars

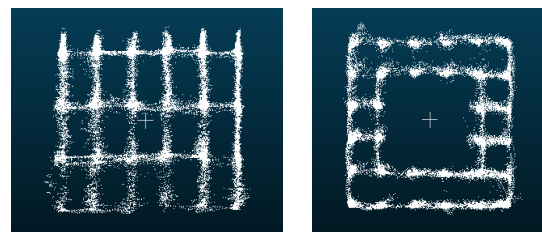
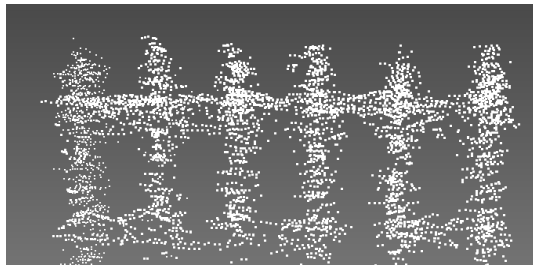
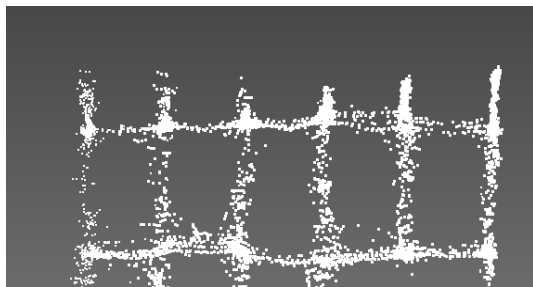


Figure 4.2 Result of Thinning Process

Fig. 4.3, 4.4 show enlarged images of the upper part and the bottom part of the result of thinning respectively.



(a) Point cloud of reinforced bars



(b) Result of Thinning Process

Figure 4.3 Enlarged view of upper part



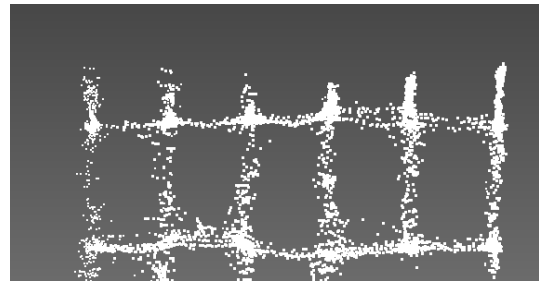
(a) Point cloud of reinforced bars



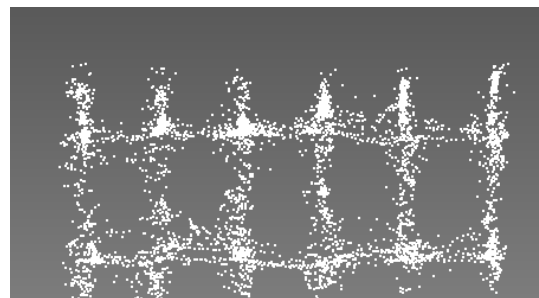
(b) Result of Thinning Process

Figure 4.4 Enlarged view of bottom part

Fig. 4.5 shows the difference between results due to the change in r .



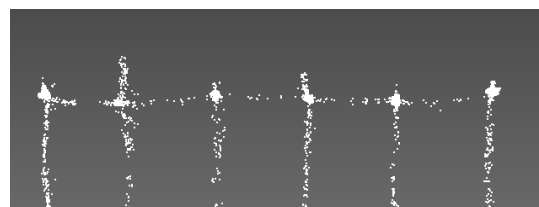
(a) $r = 10$ voxel width



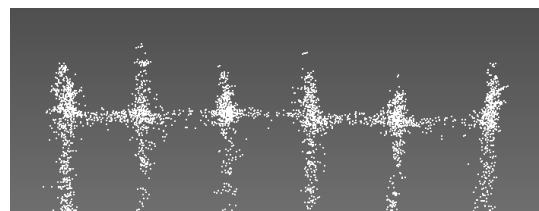
(b) $r = 5$ voxel width

Figure 4.5 Comparison of results by changing r

Furthermore, we verified the effectiveness of the countermeasure against the problem that the point cloud becomes discontinuous among the intersection points of reinforced bars. The result is shown in Fig. 4.6.



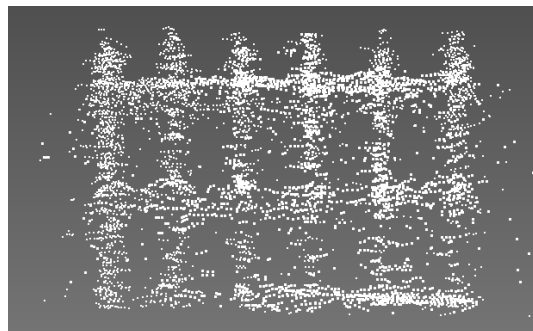
(a) Without countermeasure



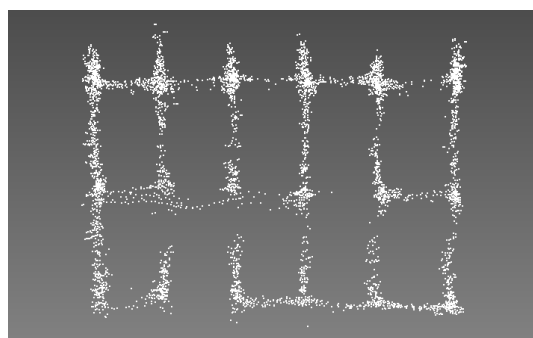
(b) With countermeasure
 $(r_s = 30\% \text{ of voxel width})$

Figure 4.6 Differences by radius r

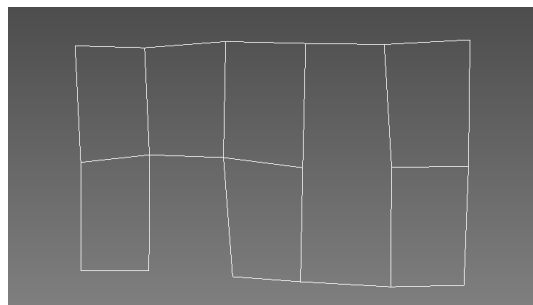
The result of core wire extraction is shown in Fig. 4.7.



(a) Point cloud of reinforced bars



(b) Result of Thinning Process



(c) Extracted core lines

Figure 4.7 Result of core line extraction

As shown in Fig. 4.2, we can see that the point cloud has been thinned. However, it can be confirmed that there is some discontinuous part. In particular, there are many discontinuities at the bottom of the data as shown in fig. 4.4. As you can see, since the distribution of point cloud is sparse, it can be seen that it is difficult to judge whether or not rebar exists by visual observation. Therefore, it is necessary to consider countermeasures by processing such as interpolation in addition to thinning.

Also, as shown in fig. 4.5, By reducing the radius of the concentration distribution, the number of convergent points increases. This is considered to be due to the fact that the influence of the density field generated from each point does not reach the surrounding points because the radius is too small, and the points does not move enough. Fig. 4.5(b) shows an example of density distribution where the size of the radius is too small.

From this result, it is considered that the size of an appropriate radius is about the radius of the reinforcing bar, but in the current method, an arbitrary value is used for the radius of the concentration distribution. Therefore, it is thought that future work is automatic parameter determination.

From Fig. 4.6, we can see the effectiveness by setting the sphere with the radius r_s . However, as introduction of this method makes it difficult for the point clusters to become thin, it is thought that it is necessary to improve so that thinning and discontinuity measures can be compatible.

As shown in Fig. 4.7, our method can extract the core wires almost correctly. However, there is some discontinuity of core wires. As a countermeasure to this problem, it is conceivable to use a different 3D scanner for scanning rebar and to change the scanning method.

5. Conclusion

In this paper, we proposed a method of extracting the core wires from the point cloud data of rebar.

In the proposed method, thinning of the point clouds of the reinforcing bars including many noises was well performed. In this thinning process, a concentration field for estimating the position of the core wire of the reinforcing bars is generated by introducing a concentration distribution function, and a vector field for converging the point cloud is constructed. Then, according to the gradient vector field, the point cloud was thinned by moving its points repeatedly. However, the convergence of the point cloud at the intersection of the reinforcing bars resulted in a problem that the point cloud where the reinforcing bars were supposed to be present occurred discontinuity. On the other hand, we considered spheres with certain radius at each point, and moved points so that spheres do not overlap and the point clouds do not concentrate to the intersection region of core wires.

In the core line extraction process, the intersection point of the reinforcing bars was detected from the generated density field, and the core line candidate of the rebar was generated from the information. When detecting the intersection point, in order to more accurately detect the intersection point, compared to the voxels existing around the current voxel, the voxel with the highest density value was taken as the

position of the intersection point of the rebar. Then, core line extraction was processed by classifying the generated core line candidates into core or non-core wires from the distribution information of the point cloud.

In the experiment, the effectiveness of core wire extraction by the proposed method was verified.

As a result, in the thinning process of the point cloud, it was possible to obtain a thinning result that suppresses the influence of noise by convergence of the point cloud.

We also confirmed how the change of each parameter influences the thinning result.

In the experiment of the core extraction process, it was confirmed that the core line can be extracted faithfully to the input data by comparing the point cloud thinning result with the core line candidates.

We think that it is necessary to perform interpolation processing when there are places where it is difficult to thin line in the input data. In addition, good processing results can be obtained by determining appropriate parameters through experiments. Therefore, it is considered that a future task is to devise a method of automatically setting parameters.

6. References

[Lee00a] Lee, In-Know, "Curve Reconstruction from Unorganized Points", *Computer Aided Geometric Design*, vol. 17, pp. 161-177, 2000.

[Luk98a] Lukács, G, Marshall, A. D., and Martin, R. R., "Geometric least-squares fitting of spheres, cylinders, cones, and tori", *ECCV '98 Proceedings of the 5th European Conference on Computer Vision-Volume I - vol.1*, pp.671-686, 1998.

[Buc09a] Bucksch, A., Lindenberg, R. C. and Mententi, M., "SkelTre - fast skeletonization for imperfect point cloud data of botanic trees", *3DOR '09 Proceedings of the 2nd Eurographics conference on 3D Object Retrieval*, pp.13-20, 2009.

[Buc08a] Bucksch, A. and Lindenberg, R., "Campino - A skeletonization method for point cloud processing", *ISPRS Journal of Photogrammetry and Remote Sensing*, vol. 63, pp. 115 - 127, 2008.

[Cao10a] Cao, J. and Olson M., "Point Cloud Skeletons via Laplacian Based Contraction", *SMI '10 Proceedings of the 2010 Shape Modeling International Conference*, pp.187-197, 2010.